Satorre, MÁ.; Millán Verdú, C.; Molpeceres, G.; Luna Molina, R.; Maté, B.; Domingo Beltran, M.; Escribano, R.... (2017). Densities and refractive indices of ethane and ethylene at astrophysically relevant temperatures. Icarus. 296:179-182. doi:10.1016/j.icarus.2017.05.005

Densities and refractive indices of ethane and ethylene at astrophysically relevant temperatures

M. Á. Satorre[a], C. Millán[a], G. Molpeceres[b], R. Luna[a], B. Maté[b], M. Domingo[a], R. Escribano[b], C. Santonja[a]

[a] *Centro de Tecnologías Físicas, Universitat Politècnica de València, Plaza Ferrándiz-Carbonell, 03801, Alcoy, Spain*

[b] *Instituto de Estructura de la Materia, IEM-CSIC, Serrano 123, E-28006, Madrid, Spain*

Abstract

We report the density and refractive index, at 633 nm, of ethane and ethylene ices at temperatures from 13 to 65 K, measured by double laser interferometry and a cryogenic quartz crystal microbalance in a high vacuum chamber. Both quantities rise with the temperature of deposition from 13 K up to a plateau, 40 K for ethane and 22 K for ethylene. **An amorphous structure is suggested for temperatures below 40 K for ethane and below 20 K for ethylene. Above these temperatures, 40 K for ethane and 20 K for ethylene, a crystalline structure is proposed**. Ethylene results deviate from **linear growth** between 25 and 35 K, where a metastable structure is reported in the literature. Density values increase from about 0.40 to 0.60 g cm^{-3} for ethane and from about 0.45 to almost 0.65 g cm^{-3} for ethylene. The real part of the refractive index changes from about 1.27 to 1.45 for ethane and from about 1.30 to almost 1.48 for ethylene. Results are relevant especially to the outer Solar System, where the presence of these molecules is reported, and for experiments involving them.

Keywords:
Ices, mechanical properties; Ices, IR spectroscopy; Trans-neptunian objects; Experimental techniques; Organic chemistry

1. Introduction

Ethane (C_2H_6) and ethylene (C_2H_4) are detected or proposed as possible components of many objects in our **Solar System**. Ethane is found in the **spectrum** of Triton (DeMeo et al., 2010; Holler et al., 2016) and as

*Corresponding author. Tel: +34966528441
Email address: msatorre@fis.upv.es (M. Á. Satorre)

a **surface component of Trans Neptunian Objects (TNOs)**, such as Pluto (DeMeo et al., 2010; Holler et al., 2014; Grundy et al., 2016), Quaoar (Barucci et al., 2015), and Makemake (Brown et al., 2015). These last authors also include ethylene as a component on Makemake's surface. Ethane also appears in comets coming from the Kuiper Belt region and from the Oort Cloud (e.g., 17P/Holmes and 1P/Halley, respectively) (Mumma and Charnley, 2011).

Ethane and ethylene are not expected to form directly on icy Solar System surfaces or in the interstellar medium. Methane can be effectively transformed into ethane, then into ethylene and more complex molecules by many different energetic processes involving electrons, ions, UV photons, etc. (Gerakines et al., 1996; Brunetto et al., 2006; Bennett et al., 2006). The way methane is processed drives the abundance of ethane and ethylene in different **astrophysical** contexts. If the surface is irradiated, relevant mixtures must be studied as was done in Molpeceres et al. (2016, 2017) for ethane-methane and ethylene-methane mixtures. The irradiation time, compared with renewal time of the irradiated surface, determines if the ice becomes richer in these molecules or if reddish tholins derive from it. Ethane and ethylene can appear segregated from the methane because of their different sublimation temperatures or because they are formed in the atmosphere and deposited, as suggested for ethane ice on the surface of Pluto by Holler et al. (2014).

The density (ρ) and real component of the refractive index (n) are important for many reasons. For instance, the density is necessary to obtain accurate IR band strengths, hence abundances, and to estimate the ion penetration depth in irradiation experiments. The refractive index, at a wavelength in a **non-absorbing** region (at 633 nm), is necessary to obtain n and **the imaginary part of the refractive index (k)** values of the ice in an absorbing region of the spectrum (i.e., IR spectral range of astrophysical interest) by the Kramers-Kroning equation (Zanchet et al., 1983). However, the information available in the literature about refractive indices or densities of the solid phases of ethane and ethylene is scarce and does not cover the temperature range relevant in astrophysics (i.e., $\sim$ 40 K for Triton and Pluto, and lower temperatures for the interstellar medium).

Hudson et al. (2014) obtained the refractive index (at 670 nm) for ethane and ethylene vapor-deposited ices at three different temperatures that they associated with three different structures: amorphous, at 12 K for ethane and 11 K for ethylene; metastable, at 47 K and 30 K, respectively; and

crystalline, at 60 K for ethane and 45 K for ethylene. They found that the refractive index grows with increasing deposition temperature, a variation assumed to be related to changes in ice density (Satorre et al., 2013). To calculate absorbance strengths in the NIR and MIR regions, Hudson et al. (2014) used the density values determined by van Nes and Vos (1978, 1979) by X-ray diffraction at 85 K, because it was the only information available so far in the literature.

We provide in this paper a comprehensive set of measurements of densities and refractive indices for ethane and ethylene ices at astrophysically relevant temperatures ranging from 13 K to 65 K. We aim to fill the gaps in refractive index at visible wavelengths and density for this temperature range, and compare our results with the scarce previous information available. Finally we discuss the temperature dependence of these quantities with respect to the structure of the corresponding ices.

2. Experimental

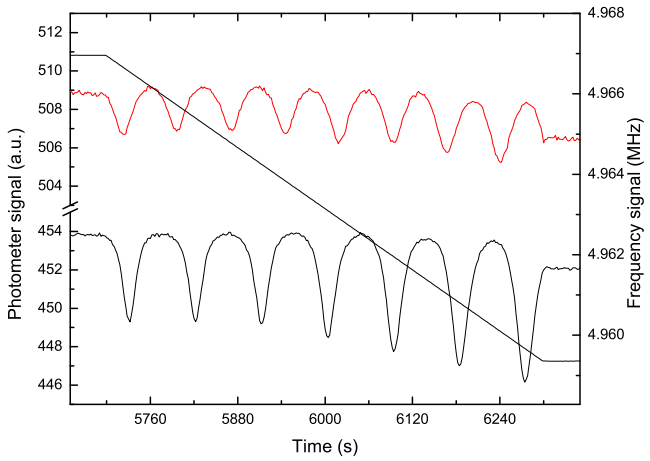

Figure 1: Ethane deposited at 45 K. **The left** axis represents laser signals at $\alpha = 33°$ (top) and $\beta = 66°$ (bottom) angles of incidence**, in arbitray units,** and **the right axis represents** the QCMB signal (the straight line) vs. time of deposition.

Experiments were performed in a setup described in detail in previous works (e.g., Satorre et al., 2013). It consists of a high vacuum (HV) chamber

at 10^{-7} mbar base pressure, inside which a closed-cycle He cryostat cools down the sample holder to 13 K. The temperature can be controlled up to room-temperature with 0.5 K accuracy. Temperatures of deposition were selected every 5 K to study the overall trend in the real part of the refractive index and the density. Below 35 K, because of higher variability in the ethylene results, deposits were grown every 2-3 K. Molecules are background-deposited onto a **gold-plated** quartz crystal microbalance (QCMB). **During deposition the pressure is maintained constant in the chamber, then a constant deposition rate is obtained. This constancy** is reflected **in** the QCMB frequency, which decreases linearly with the mass deposited (straight line in Figure 1). These parameters are related by the Sauerbrey equation ($\Delta f = -S \cdot \Delta m$). In this equation Δf is the change in frequency, Δm represents the mass accreted onto the QCMB and S is a specific constant for every QCMB. Two He-Ne laser beams (633 nm) impinge at the center of the QCMB at two angles of incidence **(α and β)**, forming two interference patterns during film growth (see Figure 1). As the thickness and the refractive index are the same for both interference patterns, and the incidence angles are known, the refractive index can be calculated as follows

$$n^2 = \frac{sin^2\beta - \gamma^2 sin^2\alpha}{1 - \gamma^2}, \tag{1}$$

where $\gamma = \frac{T_\alpha}{T_\beta}$ and $\mathbf{T}_\alpha$ **and** $\mathbf{T}_\beta$ are the periods of the corresponding angles of incidence**, measured in seconds**. Knowing the refractive index, the thickness is determined. The samples are typically a few microns (μm) in thickness. The density was calculated by dividing the mass deposited per unit area (g cm^{-2}) measured with the QCMB by the thickness (cm) determined with the lasers. Films were accreted at 1-15 μm h^{-1}. Praxair gases of purity 99.99% and 99.95% for ethane and ethylene, respectively, were used in all the experiments.

3. Results and discussion

Table 1 collects our results for n and ρ of ethane and ethylene for a temperature range of 13 K to 65 K. These results are visualized in Figure 2. The lower temperature of deposition is 13 K, the minimum our system can achieve, and the highest is 65 K, because for higher temperatures sublimation was not negligible in our HV chamber. Temperatures were selected to follow the overall trend of both molecules. Data were measured at more

Table 1: Density, ρ, and refractive index, n, of ethane and ethylene deposited at different temperatures. Uncertainties on each density and refractive index are 0.01 g cm^{-3} and 0.01, respectively.

Temperature	Ethane (C_2H_6)		Ethylene (C_2H_4)	
(K)	ρ (g cm^{-3})	n	ρ (g cm^{-3})	n
13	0.41	1.28	0.46	1.33
16	-	-	0.51	1.38
18	0.41	1.27	0.53	1.42
20	0.44	1.31	0.56	1.45
22	-	-	0.57	1.47
25	0.47	1.33	0.58	1.47
28	-	-	0.59	1.45
30	0.53	1.39	0.58	1.44
33	-	-	0.62	1.47
35	0.54	1.40	0.64	1.49
40	0.60	1.44	0.64	1.49
45	0.60	1.43	0.65	1.50
50	0.60	1.43	0.63	1.47
55	0.59	1.42	0.64	1.48
60	0.62	1.47	0.63	1.47
65	0.60	1.44	0.63	1.49

Table 2: Density, ρ, and refractive index, n, of ethane and ethylene linear fits for amorphous structure. Q = A+BT where Q is the quantity and T is the temperature of deposition in K.

Molecule	Ethane (C_2H_6)			Ethylene (C_2H_4)		
	Linear fit		Plateau	Linear fit		Plateau
T_{range}	13 - 40 K		40 - 65 K	13 - 20 K		35 - 65 K
Quantity (Q)	A	B (K^{-1})		A	B (K^{-1})	
n	1.18	0.0065	1.44	1.10	0.0177	1.48
ρ (g cm^{-3})	0.299	0.0073	0.60	0.281	0.0140	0.64

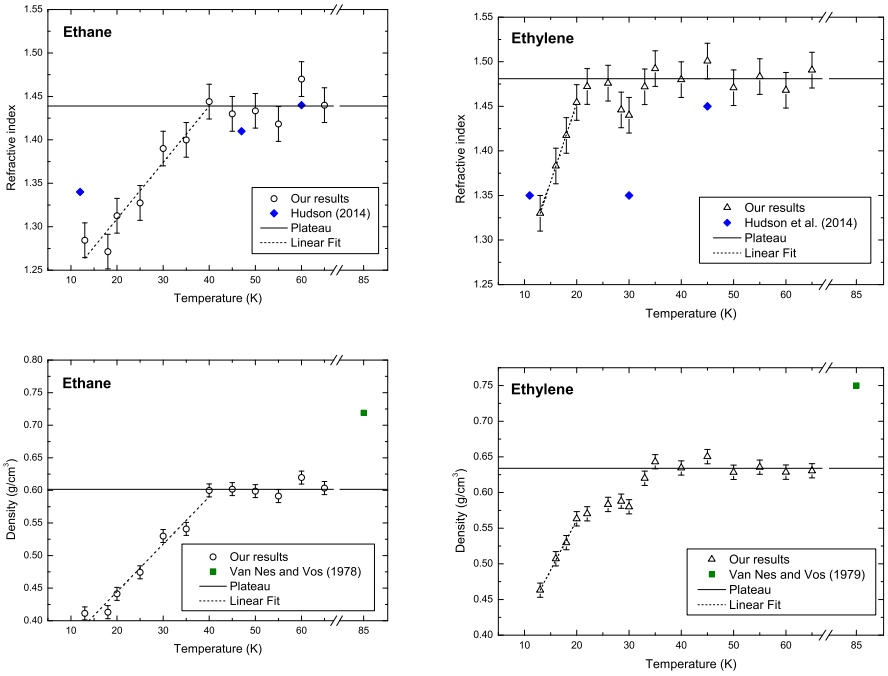

Figure 2: Refractive index, n, (top row) and density, ρ, (bottom row) for ethane (left column) and ethylene (right column) deposited at low temperatures from 13 to 65 K.

temperatures for ethylene: at 16 K because its slope is steeper than that of ethane; and between 20 and 35 **K**, because it shows a drop not present in the case of ethane. Error bars are shown for a 95% confidence interval (Student's t-distribution), obtained statistically from experiments repeated at the same temperature; seven times at 30 K for ethylene because it presents the higher variability. **We have chosen to apply the ethylene confidence interval to ethane because it is greater than that of ethane.** Refractive index and density are correlated and follow a similar trend with temperature, initially with a linear increment (linear fits appear in **Figures 1 and 2; parameter values** are listed in Table 2), followed by a constant plateau (highlighted by horizontal lines in the figures). The plateau values (see Table 2) were calculated as the average of all the experiments for temperatures higher than 40 K for ethane and higher than 35 K for ethylene, where results present low variability. These temperatures are the same for both density and refractive index, relating them with structural changes as

will be discussed below.

We have included in Figure 2 refractive index values from Hudson et al. (2014), and the density values of van Nes and Vos (1978, 1979). The densities measured by van Nes and Vos (1978, 1979) are higher than our values at 65 K, probably because of the different nature of the samples. Van Nes and Vos (1978, 1979) formed perfect crystals with no pores at 85 K, whereas our ices are accreted by background vapor deposition and include voids in the structure, as has been observed in other ices (Bossa et al., 2015). **From our work and that of van Nes and Vos (1979), ethylene was found to be denser than ethane even though ethylene has lower molecular mass**. The C=C double bound shortens the distance between carbon atoms and makes the four hydrogen atoms lay in the same plane. **These factors reduce the size of the unit cell by about 10%**, as revealed by X-ray diffraction, increasing the density of ethylene with respect to ethane. However mass reduction partially balances this effect, giving a final density increase of about 5%. **Errors up to 40% can be avoided using our density values for calculating band strengths or ion penetration depths where the density is the key parameter** (i.e., $\sim$0.4 g cm^{-3} obtained by us at low temperatures compared with $\sim$0.7 g cm^{-3} used from the literature). **These errors** decrease to about 15 % for crystalline samples.

The real part of the refractive index obtained by Hudson et al. (2014), at 670 nm, can be compared with ours at 633 nm. This is because both are far from UV and IR absorption zones, and little variation is expected. For the lower temperatures their values are somewhat higher than ours for both molecules because of the different deposition procedure. Loeffler et al. (2016) proved recently that normal deposition leads to higher n values than background deposition at low temperatures (amorphous), but both procedures give the same results when an ordered structure is achieved. This explains why Hudson et al. (2014) and our results are so similar for the highest temperatures of deposition, corresponding to the crystalline stable structure. There is a stark disagreement for ethylene at 30 K which we will comment on below.

Our results provide information on the structure of ethane and ethylene. Based on previous studies **(Wisnosky et al., 1983; Hudson et al., 2014)**, there are two different temperature ranges associated with the amorphous and crystalline structures. At low temperatures, an amorphous structure shows n and ρ values increasing with the temperature of deposition up to 40 K for ethane and 20 K for ethylene. For higher temperatures of deposition,

two types of crystalline structures appear: a stable one at the highest temperatures of deposition, and another metastable **one** between the amorphous and the stable crystalline structures. The latter is labeled **"metastable"** because it is formed when depositing at certain temperatures but not by warming up the amorphous structure. The stable crystalline form, however, can be obtained **by** depositing at high temperatures or warming up the other structures.

For ethane, Hudson et al. (2014) assumed a metastable structure at 47 K and the crystalline one at 60 K, with **comparable** refractive index values **for** each structure. **Also**, Wisnosky et al. (1983) conclude that the metastable phase "must be ordered and crystalline, rather than disordered or glassy." We find nearly constant values (within the error bars) of both refractive index and density of ethane within the plateau region, which supports the idea that the metastable and crystalline structures may not be too different, **in agreement with Wisnosky et al. (1983) and Hudson et al. (2014)**. Ethylene, on the **other hand**, shows **significant** differences **in** the n and ρ values for both phases. The dip ethylene presents in the 22-35 K range might indicate this metastable phase presents more defects in its structure than that of ethane, making them different in nature. Additionally, it seems to be sensitive to variation in the generation conditions. Hudson et al. (2014) deposited at 60 μm h^{-1} to make this phase, and 1 μm h^{-1} for the other experiments. It may be argued that this is the reason for **the** low value of the refractive index of ethylene at 30 K.

Both molecules take amorphous structures at low deposition temperatures, displaying higher n and ρ values as the temperature of deposition increases. Ethane presents this amorphous structure for a wider range of temperature from 13 K to 40 K. Ethylene shows a narrower range from 13 K to 20 K with steeper variations. **This increase indicates a more compact structure, but ethylene is still in the amorphous phase until the metastable structure is formed.**

4. Conclusions

In this work we provide visible refractive indices and densities of ethane and ethylene ices at astrophysically relevant temperatures, from 13 K to 65 K (Table 1 and Figure 2). These parameters are essential to obtain optical constants in the infrared, ice thickness in laboratory experiments, band

strengths, ion penetration depths, **and** relative buoyancy in geological processes, among other physical and chemical **processes**.

We can make inferences about the structure of the ices from our result of n and ρ obtained at different temperatures of deposition. Ethane shows two structures: amorphous, from 13 to 40 K, and crystalline for higher temperatures of deposition. Neither the density nor the refractive index vary between the metastable and stable crystalline **phases**, in agreement with Hudson et al. (2014) and Wisnosky et al. (1983). Ethylene shows three different phases: amorphous (up to 20 K); metastable crystalline (22-35 K); and stable crystalline (for higher deposition temperatures). For both species, the amorphous structures become denser and reveal increasing n values with higher temperatures of deposition. Our results agree with the structural study by IR spectroscopy (Hudson et al., 2014).

Up to now, the only density data available in the literature for these ices refers to perfect crystals formed at 85 K (van Nes and Vos, 1978, 1979). These ices may be quite different than those generated in the present work, **which were** prepared in conditions that mimic astrophysical environments. Use of the previous density values for astrophysical ices could lead to inaccuracies.

The present results are meant for applications in astrophysical contexts and their representative temperatures. Thus, data for the lowest temperatures are relevant to the interstellar medium; those for intermediate ones, to the outer Solar System bodies such as TNOs; and those at the highest temperatures for objects closer to the Sun, such as comets during their perihelion.

In the last fifteen years, high signal-to-noise spectra (e.g., Brown et al., 2015), patient observational campaigns **(e.g., Holler et al., 2014)**, and spacecraft flyby observations (Stern et al., 2015) have enabled the detection of ethane and ethylene in the outer Solar System. The results presented here are expected to be relevant for the study of such observational data. Additionally, as both molecules are products of methane energetic processing (e.g., Gerakines et al., 1996; Brunetto et al., 2006; Bennett et al., 2006), results will be useful where methane has been detected and its evolution is expected. As new observational facilities become available (i.e., JWST) it would be possible to detect these molecules in many different contexts, in addition to those where they have already been detected. In this way, our results provide even more valuable data to apply to observations, simulations**,** and laboratory studies.

Acknowledgments

The authors would like to thank the two reviewers for their comments that certainly improve this paper in content and form. This work was supported by the Ministerio de Economía y Competitividad FIS2013-48087-C2-2-P, FIS2013-48087-C2-1-P, and AYA2015-71975-REDT.

References

Barucci, M.A., et al., 2015. (50000) Quaoar: Surface composition variability. Astron. Astrophys. 584, A107, 7 pp.

Bennett, C.J., Jamieson, C.S., Osamura, Y., Kaiser, R.I., 2006. Laboratory studies on the irradiation of methane in interstellar, cometary, and Solar System ices. Astrophys. J. 653, 792-811.

Bossa, J.B., et al., 2015. Porosity and band-strength measurements of multi-phase composite ices. Astrophys. J. 814, 47, 14 pp.

Brown, M.E., Schaller, E.L., Blake, G.A., 2015. Irradiation products on dwarf planet Makemake. Astron. J. 149, 105, 6 pp.

Brunetto, R., Barucci, M.A., Dotto, E., Strazzulla, G., 2006. Ion irradiation of frozen methanol, methane, and benzene: Linking to the colors of centaurs and trans-Neptunian objects. Astrophys. J. 644, 646-650.

DeMeo F.E., et al., 2010. A search for ethane on Pluto and Triton. Icarus 208, 412-424.

Gerakines, P.A., Schutte, W.A., Ehrenfreund, P., 1996. Ultraviolet processing of interstellar ice analogs. I. Pure ices. Astron. Astrophys. 312, 289-305.

Grundy, W.M., et al., 2016. Surface compositions across Pluto and Charon. Science 351, aad9189.

Holler, B.J., Young, L.A., Grundy, W.M., Olkin, C.B., Cook, J.C., 2014. Evidence for longitudinal variability of ethane ice on the surface of Pluto. Icarus 243, 104-110.

Holler, B.J., Young, L.A., Grundy, W.M., Olkin, C.B., 2016. On the surface composition of Triton's southern latitudes. Icarus 267, 255-266.

Hudson, R.L., Gerakines, P.A., Moore, M.H., 2014. Infrared spectra and optical constants of astronomical ices: II. Ethane and ethylene. Icarus 243, 148-157.

Loeffler, M. J., Moore, M. H., Gerakines, P. A., 2016. The effects of experimental conditions on the refractive index and density of low-temperature ices: solid carbon dioxide. Astrophys. J. 827, 98, 7 pp.

Molpeceres, G., et al., 2016. Optical constants and band strengths of CH_4:C_2H_6 ices in the Near- and mid- Infrarred. Astrophys. J. 825, 156, 12 pp.

Molpeceres, G., et al., 2017. Physical and spectroscopic properties of pure C_2H_4 and CH_4:C_2H_4 ices. Mon. Not. R. Astron. Soc. 466, 1894-1902.

Mumma, M.J., Charnley, S.B., 2011. The chemical composition of comets-emerging taxonomies and natal heritage. Annu. Rev. Astron. Astrophys. 49, 471-524.

Satorre, M.Á., Leliwa-Kopystynski, J., Santonja, C., Luna, R., 2013. Refractive index and density of ammonia ice at different temperatures of deposition. Icarus 225, 703-708.

Stern, S.A., et al., 2015. The Pluto system: Initial results from its exploration by New Horizons. Science 350, add1815.

van Nes, G.J.H., Vos, A., 1978. Single-crystal structures and electron density distributions of ethane, ethylene and acetylene. I Single-Crystal X-ray structure determinations of two modifications of ethane. Acta Crys. B34, 1947-1956.

van Nes, G.J.H., Vos, A., 1979. Single-crystal structures and electron density distributions of ethane, ethylene and acetylene. III Single-Crystal X-ray structure determination of ethylene at 85 K. Acta Crys. B35, 2593-2601.

Wisnosky, M.G., Eggers, D.F., Fredrickson, L.R., Decius, J.C., 1983. A metastable solid phase of ethane. J. Chem. Phys. 79, 3513-3516.

Zanchet, A., Rodríguez-Lazcano, Y., Gálvez, Ó., Herrero, V.J., Escribano, R., Maté, B., 2013. Optical constants of NH_3 and NH_3:N_2 amorphous ices in the near-infrared and mid-infrared regions. Astrophys. J. 777, 26, 11 pp.